EJN fens EUROPEAN JOURNAL OF NEUROSCIENCE

European Journal of Neuroscience, pp. 1–14, 2013 doi:10.1111/ejn.12433

Mechanisms underlying the basal forebrain enhancement of top-down and bottom-up attention

Michael C. Avery,[1] Nikil Dutt[2] and Jeffrey L. Krichmar[1,2]
[1]Department of Cognitive Sciences, University of California, 2224 Social and Behavioral Sciences Gateway, Irvine, CA 92697-5100, USA
[2]Department of Computer Sciences, University of California, Donald Bren School of Information and Computer Sciences, Irvine, CA 92697-3435

Keywords: computational model, correlated firing, neuromodulation, vision

Abstract

Both attentional signals from frontal cortex and neuromodulatory signals from basal forebrain (BF) have been shown to influence information processing in the primary visual cortex (V1). These two systems exert complementary effects on their targets, including increasing firing rates and decreasing interneuronal correlations. Interestingly, experimental research suggests that the cholinergic system is important for increasing V1's sensitivity to both sensory and attentional information. To see how the BF and top-down attention act together to modulate sensory input, we developed a spiking neural network model of V1 and thalamus that incorporated cholinergic neuromodulation and top-down attention. In our model, activation of the BF had a broad effect that decreases the efficacy of top-down projections and increased the reliance of bottom-up sensory input. In contrast, we demonstrated how local release of acetylcholine in the visual cortex, which was triggered through top-down gluatmatergic projections, could enhance top-down attention with high spatial specificity. Our model matched experimental data showing that the BF and top-down attention decrease interneuronal correlations and increase between-trial reliability. We found that decreases in correlations were primarily between excitatory–inhibitory pairs rather than excitatory–excitatory pairs and suggest that excitatory–inhibitory decorrelation is necessary for maintaining low levels of excitatory–excitatory correlations. Increased inhibitory drive via release of acetylcholine in V1 may then act as a buffer, absorbing increases in excitatory–excitatory correlations that occur with attention and BF stimulation. These findings will lead to a better understanding of the mechanisms underyling the BF's interactions with attention signals and influences on correlations.

Introduction

Attention can selectively sharpen or filter sensory information on a moment by moment basis. We typically separate attention into two distinct categories: bottom-up (sensory driven) and top-down (goal-directed) (Desimone & Duncan, 1995; Buschman & Miller, 2007). The cholinergic system, which originates in the basal forebrain (BF), has been shown to be important for enhancing bottom-up sensory input to the cortex at the expense of intracortical interactions and enhancing cortical coding by decreasing noise correlations and increasing reliability (Hasselmo & McGaughy, 2004; Yu & Dayan, 2005; Disney *et al.*, 2007; Goard & Dan, 2009). Herrero *et al.* (2008), however, have recently found that acetylcholine is also important for top-down attentional modulation. It is still unclear exactly how the BF may be important for facilitating *both* top-down attentional and bottom-up sensory input into the visual cortex.

Top-down attention is usually associated with an increase in firing rate in the set of neurons coding for a particular feature (Desimone & Duncan, 1995). This effectively biases that feature over other competing features. Recent experimental studies, however, have shown that attention causes changes in the variability of neural responses within and between trials (Cohen & Maunsell, 2009; Mitchell *et al.*, 2009; Harris & Thiele, 2011; Herrero *et al.*, 2013). This implies that interactions between neurons are a critical factor for encoding information in sensory cortex.

We present a spiking neuron model that simulates the effects that top-down attention and the BF have on visual cortical processing. We show an increase in between-trial correlations and a decrease in between-cell correlations in the cortex via GABAergic projections to the thalamic reticular nucleus (TRN) and cholinergic projections onto muscarinic acetylcholine receptors (mAChRs) in the primary visual cortex (V1), respectively. In addition, we show that topographic projections from attentional areas to the TRN can increase reliability of sensory signals before they get to the cortex (Fig. 1). We demonstrate that GABAergic projections from the BF to the TRN are a means by which the BF can effectively 'wash out' top-down attentional filters that act on the thalamus, thus providing a new mechanism for BF's control of bottom-up and top-down information. Local mAChR activation via top-down attentional signals is also important in our model for facilitating top-down attention in V1 and helps to both

Correspondence: Dr M. C. Avery, as above.
E-mail: averym@uci.edu

Received 28 March 2013, revised 11 October 2013, accepted 25 October 2013

increase the firing rate and decrease noise correlations between these neurons (Herrero *et al.*, 2008; Goard & Dan, 2009). Specifically, our model highlights how mAChR stimulation of excitatory neurons is important for attentional modulation while mAChR stimulation of inhibitory neurons is important for maintaining low levels of excitatory–excitatory correlations when excitatory drive is increased.

Contrary to recent experimental studies, which suggest a decrease in excitatory–excitatory correlations between neurons with BF stimulation and top-down attention, our model indicates that attention and mAChR stimulation in V1 lead to a decrease in excitatory–inhibitory correlations, but cause no change in excitatory–excitatory correlations. Thus, because it is difficult to distinguish between excitatory and inhibitory neurons experimentally (Nowak *et al.*, 2003; Vigneswaran *et al.*, 2011), it is possible that experimenters are seeing excitatory–inhibitory rather than excitatory–excitatory decorrelations. This is a strong prediction of our model. We suggest inhibition may act as a mechanism for absorbing additional excitatory input that may result from increased excitatory drive from top-down attentional signals or activation of mAChRs on excitatory neurons in order to extinguish excess excitatory–excitatory correlations.

Methods

A model was developed that contained two cortical columns, simulating two receptive fields, and was subject to both neuromodulation by the BF and top-down attention (see Fig. 3). Input to the model was a movie of a natural scene as described below. Our goal was to see how neuromodulatory and top-down attention signals interacted and influenced between-trial and between-neuron correlations in the simulated cortical columns.

Stimuli presentation and pre-processing

Our experiment consisted of 60 trials, in which a 12-s natural scene video was input to the spiking neural network. We used this natural stimulus because it is similar to that used in Goard & Dan's (2009) experiments and affords comparison of our model's responses with their results. The video was obtained from the van Hateren movie database to the network (http://biology.ucsd.edu/labs/reinagel/pam/NaturalMovie.html). Experiments consisted of six blocks of ten trials (see Fig. 2A). In each block of ten trials, five were performed without BF stimulation, top-down attention and/or mAChR stimulation

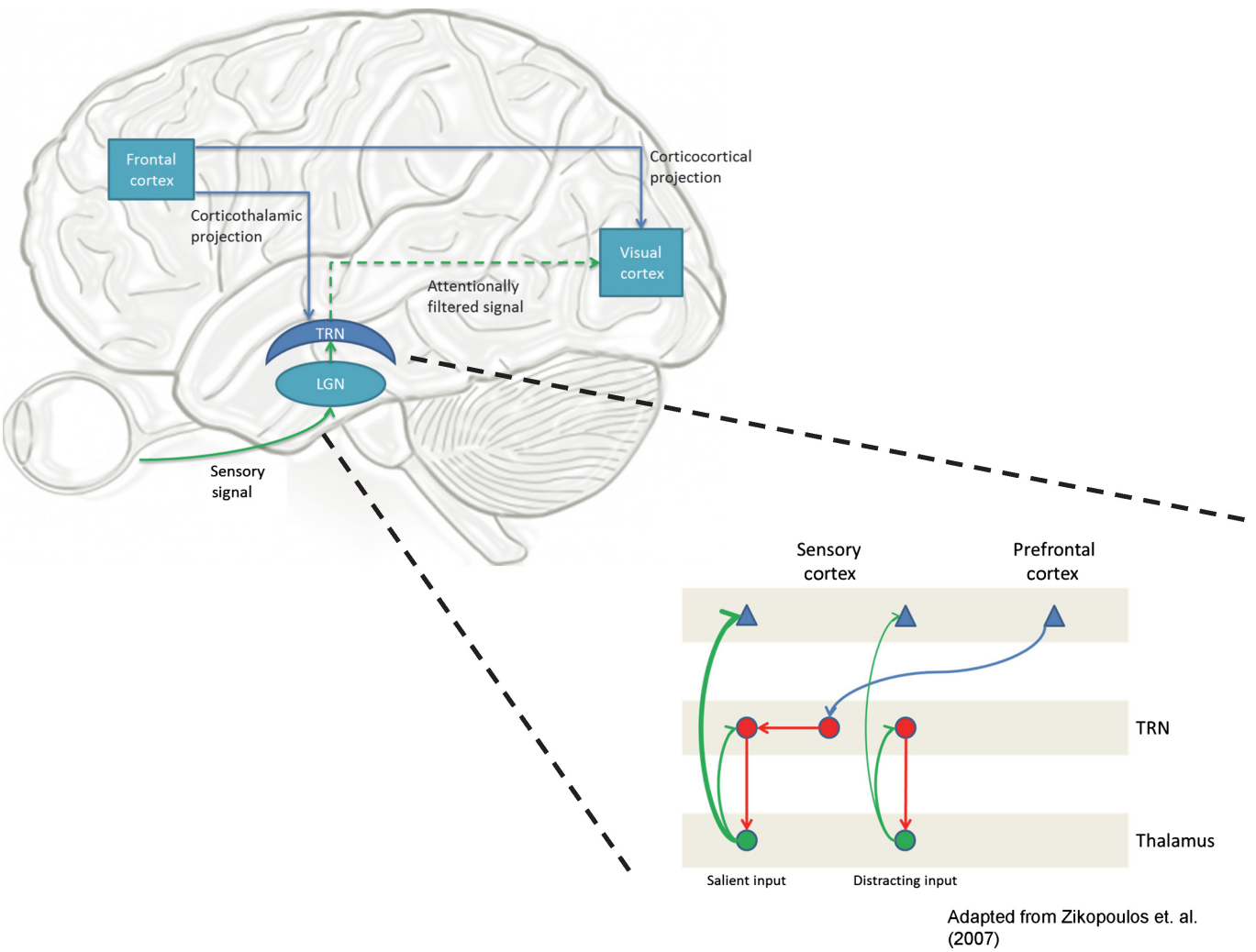

FIG. 1. Frontal corticocortical and corticothalamic projections. Schematic diagram showing how frontal areas may influence sensory information directly via direct corticocortical connections or via projections to the thalamic reticular nucleus (TRN), before the information is able to get to the cortex. The architecture was adapted from Zikopoulos & Barbas (2007), who showed that there are topographic projections from the frontal cortex to the TRN that may be able to selectively enhance one input and dampen another.

(control) followed by five trials with BF stimulation, top-down attention and/or mAChR stimulation (non-control). In between each trial and block, 1 and 4 s, respectively, of random, Poissonian spikes was injected into the network at a rate of 2 Hz to allow network activity to settle. The total simulation time of the experiment was 13.4 min. This took approximately 78 min to run on a Tesla M2090 GPU.

The video contained 300 frames and each frame was presented to the model for 40 ms of simulation time. Each image was originally 256 × 256 pixels. Because our cortical model is made up of single columns, however, the input size was reduced to 20 × 20 pixels (see Fig. 2B) to approximate the visual space that would drive neurons in a receptive field of a V1 cortical column. This was an assumed approximation given the 100 deg^2 receptive field and 36 × 36 (64 × 64 pixel) input from the Goard and Dan experiment. In the 256 × 256 pixel image, RF1 received input from pixels (121–140) × (121–140) and RF2 received input from pixels (141–160) × (121–140). Figure 3 shows the architecture of RF1 and RF2.

It has been shown that retinal neurons remove linear correlations by 'whitening' images before they reach the cortex (Simoncelli & Olshausen, 2001). To simulate this, all the images were whitened and normalised before being presented to the network (Fig. 2B). Whitening was achieved by applying a Gaussian filter to the Fourier-transformed image (see http://redwood.berkeley.edu/bruno/npb261b/). This flattens the power spectrum of the image and is essentially equivalent to convolving the image with an on-center off-surround filter, as is observed in retinal ganglion cells and the lateral geniculate nucleus (LGN). As we were not interested in modeling orientation selectivity development, we assumed that the simulated V1 columns, RF1 and RF2, were selective to vertical edges. Therefore, the images were convolved with a vertical Gabor filter after whitening. The Gabor filter was constructed by modulating a Gabor kernel with a sinusoidal wave as shown in Eqn. (1), where σ_x and σ_y determine the spatial extent of the Gaussian in x and y and f specifies the preferred spatial wavelength (Dayan & Abbott, 2001). Excitatory Poisson spike generators converted the images into spike trains in the input layer.

$$G(x,y) = \frac{1}{2\pi\sigma_x\sigma_y}\exp\left(-\frac{x^2}{2\sigma_{x^2}} - \frac{y^2}{2\sigma_{y^2}}\right)\sin\left(\frac{2\pi}{f}x\right) \qquad (1)$$

Network model

To develop our model, we used a publicly available simulator, which has been shown to simulate large-scale spiking neural networks efficiently and flexibly (Richert *et al.*, 2011). The model contained a TRN, LGN, BF, two prefrontal cortex areas (providing top-down attention) and two, four-layered cortical microcircuits (Fig. 3). The cortical microcircuit architecture was adapted from Wagatsuma *et al.* (2011), which was able to account for experimental observations of attentional effects on visual neuronal responses and showed that top-down signals enhanced responses in layers 2/3 and 5.

All connections that occur between layers in a microcircuit are shown in Fig. 3. Within each layer, there are excitatory–excitatory, excitatory–inhibitory, inhibitory-excitatory and inhibitory–inhibitory

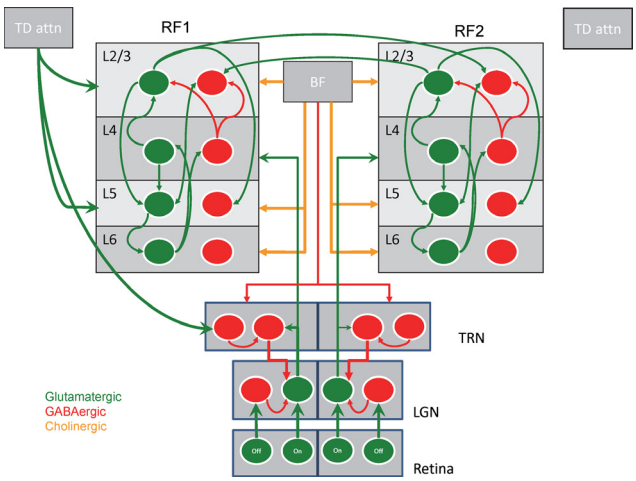

FIG. 3. Network model. The model contained a neuromodulatory area (BF), two prefrontal cortex areas (providing top-down attention) and two, four-layered cortical microcircuits (RF1 and RF2), each of which had a subcortical area composed of an input, TRN and LGN. The cortical microcircuit architecture was adapted from Wagatsuma *et al.* (2011). All connections that occur between layers in a microcircuit are shown above. Within each layer, there are excitatory–excitatory, excitatory–inhibitory, inhibitory–excitatory and inhibitory–inhibitory connections (not shown).

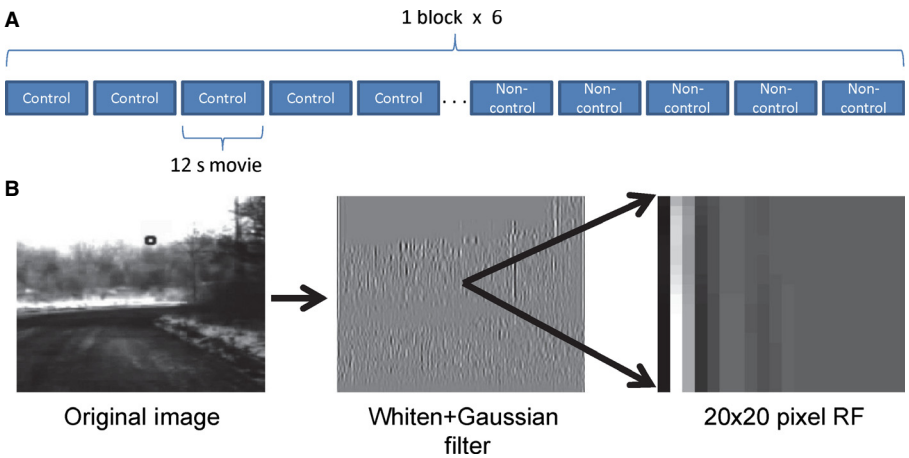

FIG. 2. Image preprocessing. (A) The experiment was divided into six blocks, with ten trials in each block. In each trial, a 12-s video (300 frames) of a natural scene from the van Hateren movie database was presented to the network. Within a block, five trials were performed under the control condition, followed by five trials for the non-control condition (mAChR stimulation, BF stimulation and/or top-down attention). (B) Each image was originally 256 × 256 pixels. Before being presented to the model, all images were first whitened and convolved with a vertical Gaussian filter. Because our cortical model is made up of single columns, however, the input size was reduced to 20 × 20 pixels to approximate the visual space that would drive neurons in a single receptive field.

TABLE 1. Cortical connection probabilities

	From							
To	L2/3e	L4e	L5e	L6e	L2/3i	L4i	L5i	L6i
L2/3e	0.1184	0.0846	0.0323	0.0076	0.1552	0.0629	0.0000	0.0000
L4e	0.0077	0.0519	0.0067	0.0453	0.0059	0.1453	0.0003	0.0000
L5e	0.1017	0.0411	0.0758	0.0204	0.0622	0.0057	0.3765	0.0000
L6e	0.0156	0.0211	0.0572	0.0401	0.0066	0.0166	0.0197	0.2252
L2/3i	0.1008	0.0363	0.0755	0.0042	0.1371	0.0515	0.0000	0.0000
L4i	0.0691	0.1093	0.0033	0.1057	0.0029	0.1597	0.0000	0.0000
L5i	0.0436	0.0209	0.0566	0.0086	0.0269	0.0022	0.3158	0.0000
L6i	0.0364	0.0034	0.0277	0.0658	0.0010	0.0005	0.0080	0.1443

TABLE 2. Number of neurons in each area of the network

Neural area	Excitatory neurons	Inhibitory neurons	Cholinergic neurons
Input	400	400	–
Subcortical			
LGN	220	–	–
TRN	–	220	–
BF	–	220	220
Cortical			
Layer 2/3	5170	1458	–
Layer 4	5478	1369	–
Layer 5	1212	266	–
Layer 6	3698	737	–

connections (data not shown). Connection probabilities in our cortical model were the same as used in Wagatsuma *et al.* (2011) and are given in Table 1. All subcortical and top-down connection probabilities were set to 0.1 except LGN excitatory to L4 excitatory ($P = 0.15$), LGN excitatory to L4 inhibitory ($P = 0.0619$), and TRN inhibitory to LGN excitatory ($P = 0.3$). The number of neurons in each area is shown in Table 2. The model contained a total of 46 926 neurons and approximately 43 million synapses.

Neuron model

Simple and extended versions of the Izhikevich model were used to govern the dynamics of the spiking neurons in this simulation. The computational efficiency of these point neurons (single compartment) makes them ideal for large-scale simulations. Izhikevich neurons are also highly realistic and are able to reproduce at least 20 different firing modes seen in the brain, which include: spiking, bursting, rebound spikes and bursts, subthreshold oscillations, resonance, spike frequency adaptation, spike threshold variability, and bistability of resting and spiking states (Izhikevich, 2004). Inhibitory and excitatory neurons in the cortex were modeled using the simple Izhikevich model, which are described by the following equations (Izhikevich, 2003):

$$\dot{v} = 0.04v^2 + 5v + 140 - u + I \tag{2}$$

$$\dot{u} = a(bv - u) \tag{3}$$

$$\text{if } v = 30, \text{then } v = c, u = u + d \tag{4}$$

where v is the membrane potential, u is the recovery variable, I is the input current, and a, b, c and d are parameters chosen based on

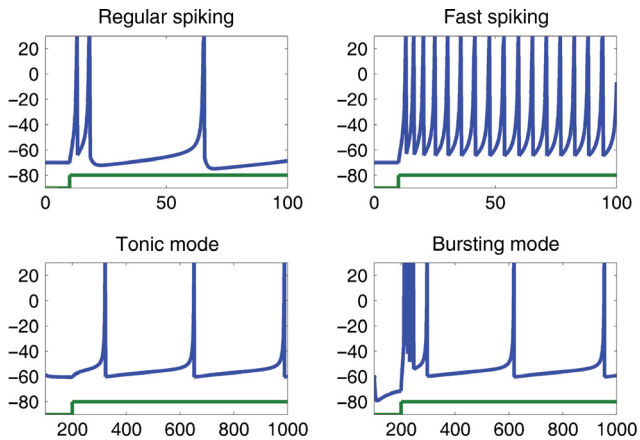

FIG. 4. Spike trains. (Top) Spike trains for regular spiking excitatory neurons (left) and fast spiking inhibitory neurons (right). (Bottom) Spike trains for thalamic neurons that may be in tonic (left) or bursting (right) mode depending on their membrane potential. If $v < -65$, the neurons are in bursting mode; otherwise, they are in tonic mode (see Methods for details).

the neuron type. For regular spiking, excitatory neurons, we set $a = 0.01$, $b = 0.2$, $c = -65.0$ and $d = 8.0$ (see Fig. 4). For fast-spiking, inhibitory neurons, we set $a = 0.1$, $b = 0.2$, $c = -65.0$ and $d = 2.0$ (Fig. 4). GABAergic and cholinergic neurons in the BF were modeled as simple Izhikevich inhibitory and excitatory neurons, respectively.

LGN and TRN neurons were modeled using the extended version of the Izhikevich neuron model to account for the bursting and tonic modes of activity, which these neurons have been shown to exhibit (Izhikevich & Edelman, 2008). The equations governing these neurons are given as:

$$C\dot{v} = k(v - v_r)(v - v_t) - u + I \tag{5}$$

$$\dot{u} = a[b(v - v_r) - u] \tag{6}$$

The equations for this extended model are similar to the previous model, except they include additional parameters, such as: membrane capacitance (C), resting potential (v_r) and instantaneous threshold potential (v_t). For LGN neurons, parameters were set to: $a = 0.1$, $c = -60$, $d = 10$, $C = 200$, $v_r = -60$ and $v_t = -50$. For TRN neurons, parameters were set to: $a = 0.015$, $c = -55$, $d = 50$, $C = 40$, $v_r = -65$ and $v_t = -45$ (Izhikevich & Edelman, 2008). To simulate the switch between bursting and tonic mode, the b parameter, which is related to the excitability of the cell, was changed

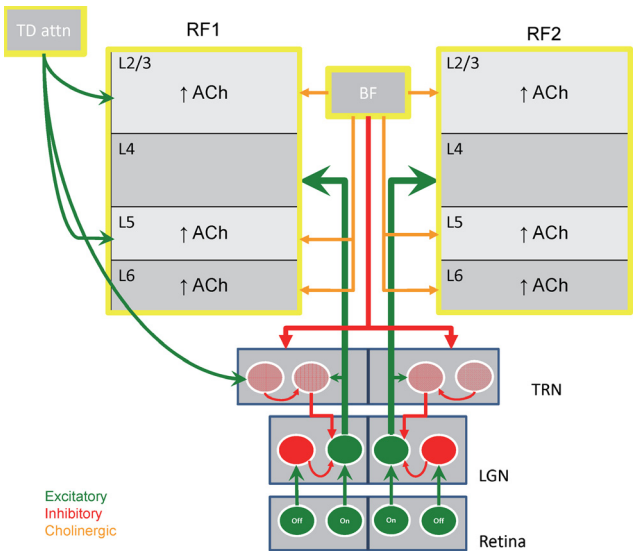

FIG. 5. Effects of basal forebrain (BF) stimulation on the network. This figure demonstrates how the network is affected when the BF is stimulated. As shown above, cholinergic projections to both RF1 and RF2 lead to increases in ACh in these columns in layers 2/3, 5 and 6. Additionally, GABAergic projections from the BF inhibit the TRN, which disinhibits the LGN and increases the efficacy of the connections from the sensory periphery to the cortex. Note also that these GABAergic connections from the BF block the top-down attentional signal on the TRN, which would otherwise be gating in information only to RF1.

depending upon membrane potential, v. Specifically, if $v < -65$, b was set to 70 and the neuron would be in bursting mode (Fig. 4; bottom, right). If $v > -65$, b was set to 0 and the neuron would be in tonic mode (Fig. 4; bottom, left).

Conductance model

The synaptic input, I, driving each neuron was dictated by simulated AMPA, NMDA, $GABA_A$ and $GABA_B$ conductances (Izhikevich & Edelman, 2008; Richert *et al.*, 2011). The conductance equations used are well established and have been described in Dayan & Abbott (2001) and Izhikevich *et al.* (2004). The total synaptic input seen by each neuron was given by:

$$I = g_{\mathrm{AMPA}}(v-0) + g_{\mathrm{NMDA}}\frac{\left[\frac{v+80}{60}\right]^2}{1+\left[\frac{v+80}{60}\right]^2}(v-0) + g_{\mathrm{GABA_A}}(v+70) + g_{\mathrm{GABA_B}}(v+90) \tag{7}$$

where v is the membrane potential and g is the conductance. The conductances change according to the following first-order equation:

$$\dot{g}_i = -\frac{g}{\tau_i} \tag{8}$$

where τ_i = 5, 100, 6 and 150 ms for i = AMPA, NMDA, $GABA_A$ and $GABA_B$ conductances, respectively. When an excitatory (inhibitory) neuron fires, g_{AMPA} and g_{NMDA} ($g_{\mathrm{GABA_A}}$ and $g_{\mathrm{GABA_B}}$) increase by the synaptic weight, w, between pre- and post-synaptic neurons.

Modulation of cortical and subcortical structures

The simulated BF modulated activity in the network in two ways (Figs 5 and 6). First, in trials in which the BF was stimulated, excitatory Poisson spike trains drove GABAergic neurons within the BF. These GABAergic neurons projected from the BF to the TRN, inhibiting GABAergic neurons in the TRN. This in turn released TRN inhibition of LGN. Second, cholinergic projections from BF to excitatory and inhibitory neurons in the cortical microcircuits were

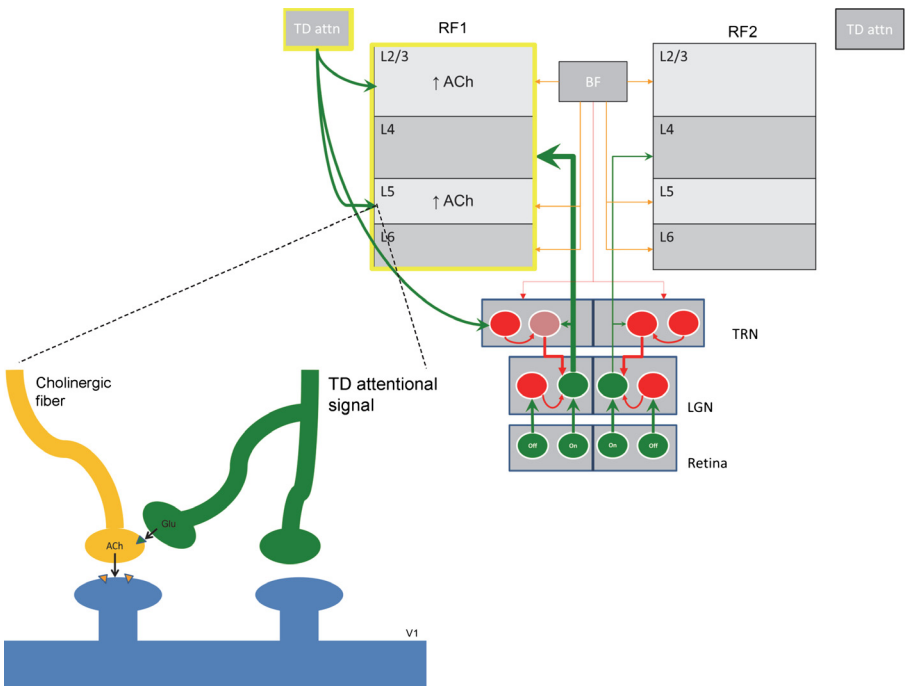

FIG. 6. Effects of attentional signals on the network. This figure demonstrates how top-down attentional signals can enhance information flow from the periphery for a single receptive field (RF1) at the thalamic level and how top-down attentional signals can cause local ACh release, which leads to a further enhancement of attention. As shown above, local ACh release happens as a result of Glu→ACh interactions. That is, glutamate release from top-down attentional fibers causes cholinergic fibers to release ACh, leading to a local cholinergic effect on V1 neurons that contain ACh receptors.

simulated. It has been shown that mAChRs tend to be localised on excitatory and inhibitory neurons in the visual cortex and are likely to increase their excitability (McCormick & Prince, 1986; Disney *et al.*, 2006). The *b* parameter in the Izhikevich equations describes the sensitivity of the recovery variable *u* to subthreshold fluctuations of the membrane potential *v* (Izhikevich, 2003). Increasing the *b* parameter decreases the firing threshold of neurons. In this sense, increasing *b* increases the cell's excitability. When the BF was stimulated, the *b* parameter in the Izhikevich model (Eqns 1 and 2), which controls cell excitability, was increased from 0.20 to 0.30 for inhibitory neurons and from 0.20 to 0.25 for excitatory neurons in layers 2, 5 and 6 of the cortical microcircuits. This is intended to mimic the cholinergic activation of mAChRs on excitatory and inhibitory neurons, which leads to increased cell excitability. Because we were mainly interested mAChR's influence on inhibitory and excitatory neurons and how it increases cell excitability, our simulation of the cholinergic system did not include the effects of nicotinic receptors on visual cortical neurons (Xiang *et al.*, 1998; Disney *et al.*, 2007). Moreover, the effects of attention probably do not affect nicotinic receptors, which are mainly expressed presynaptically on thalamocortical terminals (Disney *et al.*, 2007). Therefore, we focused on mAChRs, because of their strong influence on attentional mechanisms and correlations.

Top-down attentional signals also acted on the network in two different ways (Fig. 6). First, in trials in which the top-down attention signal projecting to RF1 was stimulated, excitatory Poisson spike trains drove GABAergic neurons within the TRN, inhibiting control of the TRN over the projections from LGN neurons that project to cortical RF1 neurons (Barbas & Zikopoulos, 2007; Zikopoulos & Barbas, 2007). This biases information coming into the cortex to RF1 over RF2. These Poisson spike trains also drove excitatory and inhibitory neurons in layers 2/3 and 5 of RF1. Second, it has been shown that local application of acetylcholine can modulate attention locally in a particular receptive field (Herrero *et al.*, 2008). A possible, although speculative, mechanism for this to occur in the brain is via glutamate (Glu) → acetylcholine (ACh) interactions as shown in Fig. 6 [proposed by Hasselmo & Sarter (2011) in the rat prefrontal cortex]. Local ACh release may help in further biasing information in early visual cortex. This was simulated in the model by stimulating mAChRs, which altered the *b* parameter (as described above) of the excitatory and inhibitory neurons that top-down signals projected to when these top-down signals were applied.

Results

The results section is organised as follows. We first demonstrate that our model matches experimental research done by Herrero *et al.* (2008) showing that the cholinergic system modulates attention in visual cortex. We then analyse the between-cell correlations and find that correlations are reduced by both top-down attention, as was seen by Cohen & Maunsell (2009) and Mitchell *et al.* (2009), and muscarinic receptor activation, as was seen by Goard & Dan (2009).

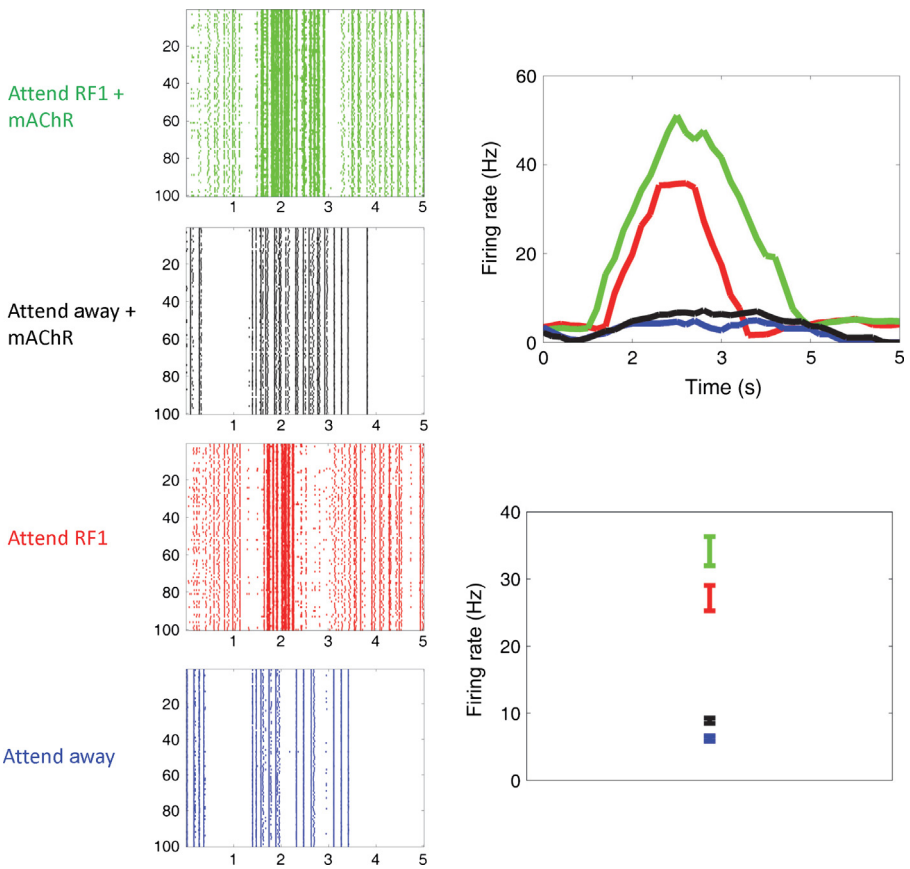

FIG. 7. Acetylcholine and attentional modulation. Rasterplot (left), mean firing rate (top, right) and average mean firing rate (bottom, right) of a subset of 100 excitatory neurons in the first 5 s of the movie presentation taken from layer 2/3 of RF1 in our model for four conditions: (i) attend RF1 + mAChR, (ii) attend away + mAChR, (iii) attend RF1 and (iv) attend away. These conditions are compared with the experimental findings found in fig. 1A of Herrero *et al.* (2008). The results from our model match well with those from Herrero *et al.* That is, the strongest response of the group of neurons in RF1 comes when both top-down attention and ACh are applied to the column and the weakest respond is when ACh is not applied and attention is directed into RF2.

In this section, we further show that these decorrelations were mediated by excitatory–inhibitory and inhibitory–inhibitory interactions and left excitatory–excitatory correlations unchanged. Finally, we analyse the between-trial correlations and demonstrate that both top-down attention and BF activation lead to increases in the between-trial correlations of excitatory neurons.

Cholinergic modulation of attention

As described in the Introduction, Herrero *et al.* (2008) performed four electrophysiological and pharmacological experiments on macaque monkeys and showed that ACh modulates attention. They had the subjects: (i) attend toward the RF that they were recording from while they applied ACh to this RF, (ii) attended away from the recorded RF while they applied ACh to the recorded RF, (iii) attend toward the recorded RF without applying ACh, and (iv) attend away from the RF without applying ACh. In the model, stimulating the frontal areas that project to RF1 and RF2, respectively, simulated the 'attend toward' and 'attend away' conditions. The ACh application condition ('mAChR' condition in Fig. 7) involved stimulating the muscarinic receptors in RF1 by increasing both the inhibitory and the excitatory cell's excitability as described in the Methods.

Our model matched results from Herrero *et al.* (2008) by showing that ACh contributes to attentional modulation. To exhibit this, we created a series of plots from our model (Fig. 7) that can be easily compared with those shown in fig. 1A of Herrero *et al.* In Fig. 7, we show raster plots, time-dependent firing rates and average firing rates for 100 excitatory neurons in layer 2/3 of RF1 for the first 5 s of the movie presentation and for the four conditions performed in Herrero *et al.* (2008). The firing rate was calculated by summing the number of spikes across the neuron population and smoothing this out using a moving average with a bin size of 100 ms. The average firing rate across time was found by computing the mean of the firing rate across neurons over the length of the trial.

The results from our model match qualitatively with those from Herrero *et al.* (2008) as can be seen in comparing Fig. 7 with fig. 1A from Herrero *et al.* That is, the strongest response of the layer 2/3 neurons in RF1 comes when both top-down attention and ACh are applied to the column and the weakest response is when ACh is not applied and attention is directed into RF2. As was speculated in Hasselmo & Sarter (2011), the attentional mechanism in our model was facilitated by the local release of ACh as a result of Glu→ACh interactions between top-down attention signals from prefrontal cortex (PFC)/V4, cholinergic fibers, and V1 neurons, as shown in Fig. 6. As explained in the Discussion and the Results below, this mAChR-mediated increase in firing rate with attention is primarily mediated by mAChR increases in the excitability of excitatory neurons, whereas the mAChR-mediated increase in excitability of inhib-

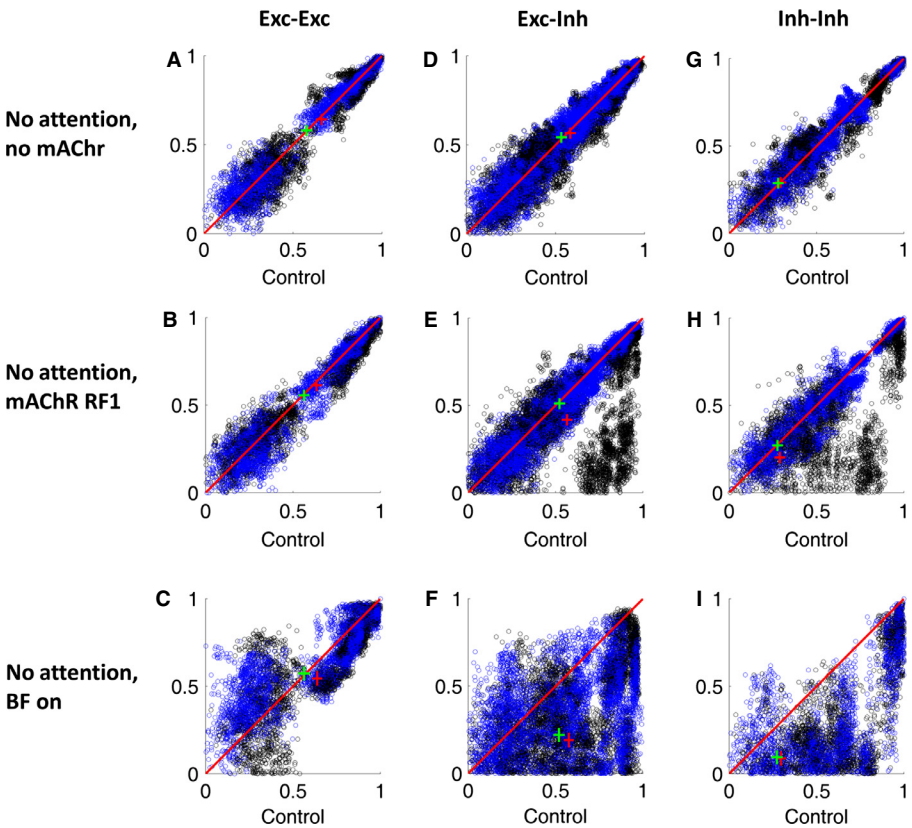

FIG. 8. Neuromodulatory effects on interneuronal correlations. Scatter plots demonstrating how mAChR and BF stimulation affect interneuronal correlations. In each case, the black and blue scatter points correspond to RF1 and RF2, respectively. The red and green crosses correspond to the center of mass of the black (RF1) and blue (RF2) scatter points, respectively (size of crosses is equal to 20× ± SEM). The left, center and right columns correspond to excitatory–excitatory, excitatory–inhibitory and inhibitory–inhibitory correlations between neurons, respectively. The top, middle and bottom rows correspond to situations in which no mAChRs are stimulated, mAChRs in RF1 are stimulated and the BF is stimulated, respectively. Note that both mAChR stimulation and BF stimulation lead to a decorrelation of excitatory–inhibitory and inhibitory–inhibitory neurons (as indicated by the red '+' below the line $y = x$) and do not significantly affect excitatory–excitatory correlations. In particular, mAChR stimulation causes excitatory–inhibitory and inhibitory–inhibitory decorrelations in RF1 only (see E and H), and BF stimulation causes excitatory–inhibitory and inhibitory–inhibitory decorrelations in RF1 and RF2 (see F and I).

itory neurons, which also occurs with top-down attention, helps to maintain low levels of excitatory–excitatory correlations. Note that the absolute changes in firing rate shown in Fig. 7 are greater than those seen in Herrero *et al.*, although this is a function of the rate that was chosen for the Poisson spike generator driving the top-down attention signal and should therefore not influence our result that mAChRs modulate attention.

In the Herrero *et al.* experiments, they found that attentional modulation was enhanced only at low doses of ACh application. Higher doses of ACh, by contrast, could reduce attentional modulation. We ran additional simulations (data not shown) showing that these results could be replicated if the excitability of inhibitory neurons increases at a faster rate than the excitability of excitatory neurons. This suggests that the number and distribution of mAChRs on excitatory and inhibitory neurons could play an important role in shaping these dose-dependent effects.

Top-down attention and BF-mediated decrease in between-cell correlation

We investigated the change in between-cell correlations that resulted from attentional and BF-related signals in comparison with control conditions. To achieve this, we periodically either stimulated top-down attentional areas, mAChRs in RF1, or the BF, as described in the Methods. This led to the six conditions shown in Figs 8 and 9: (i) no attention, no mAChR stimulation and no BF stimulation (Fig. 8, top); (ii) no attention and mAChRs in RF1 stimulated (Fig. 8, middle); (iii) no attention and BF stimulated (Fig. 8, bottom); (iv) attention signal in RF1 only (Fig. 9, top); (v) attention signal in RF1 and mAChRs in RF1 stimulated (Fig. 9, middle); and (vi) attention signal in RF1 and the BF stimulated (Fig. 9, bottom). We refer to these six cases as the 'non-control' conditions. Control conditions, by contrast, refer to times in the experiment when there was no top-down attention, no mAChR stimulation and no BF stimulation was applied to the network. We then measured the interneuronal correlations in the non-control and control conditions. This was done by first binning the spikes of all neurons at 100 ms. Binning spikes at 100 ms removes high-frequency oscillations, and thus correlations seen in the plots are low-frequency correlations. This was a similar analysis as was used in Goard & Dan (2009). We then used the MATLAB routine *corrcoef* to compute the correlation coefficient for a subset of 80 neurons taken from all layers (20 neurons per layer) in RF1 and RF2 across trials in both the control and the stimulated cases.

To see how attention, mAChR stimulation and BF stimulation changed correlations between cells, in Figs 8 and 9 we plot the excitatory–excitatory, excitatory–inhibitory and inhibitory–inhibitory correlations for the six non-control conditions discussed above (indicated by the row name). For each of the nine subplots in Figs 8 and 9, the non-control condition is plotted on the *y*-axis against the control condition, plotted on the *x*-axis. Each scatter point corresponds to the correlation value computed under both the non-control (*y*-axis) and control (*x*-axis) conditions. Thus, a scatter point above the line $y = x$ indicates an increase in correlation in the non-control

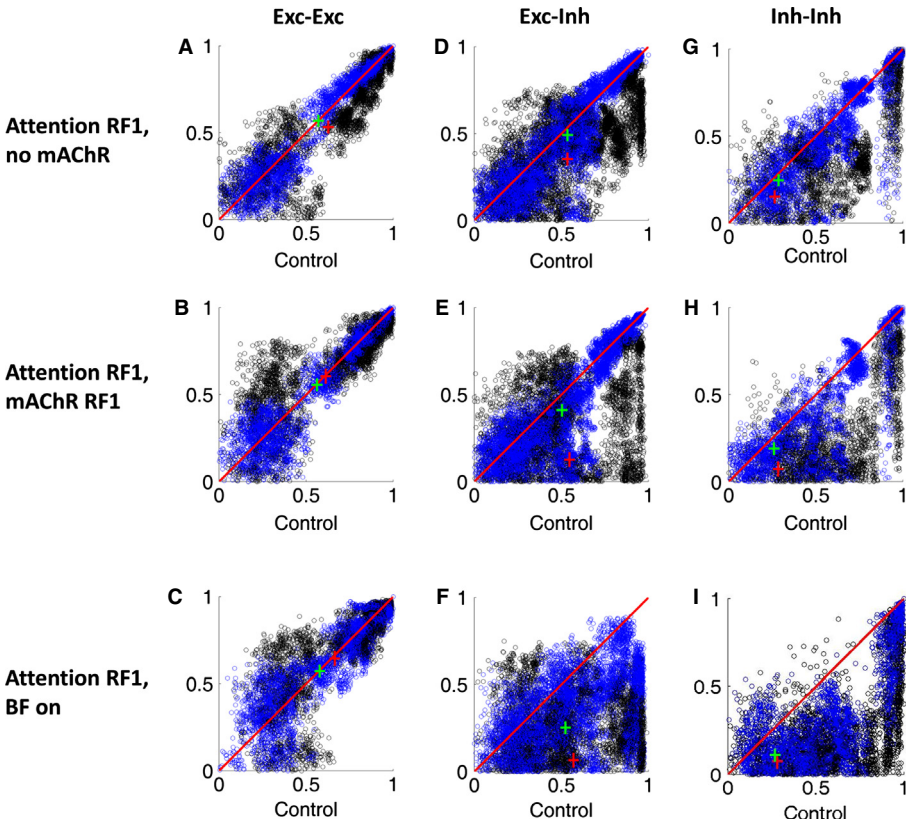

FIG. 9. Attentional and neuromodulatory effects on interneuronal correlations. Scatter plots demonstrating how top-down attention, mAChR stimulation and BF stimulation affect interneuronal correlations. As in Fig. 8, black and blue scatter points correspond to RF1 and RF2, respectively, and the red and green crosses correspond to their center of masses. When top-down attention is applied to RF1, there is a decorrelation of excitatory–inhibitory and inhibitory–inhibitory neurons (see Fig. 8D and G). The top-down attention signals also tend to further decorrelate excitatory–inhibitory and inhibitory–inhibitory neurons in combination with mAChR stimulation in RF1 (see Fig. 8E and H), indicating a strong separation from RF2. When the BF is turned on, however, this separation is diminished, as can be seen in the bottom, center and bottom, right plots, indicating a decreased bias to RF1 over RF2.

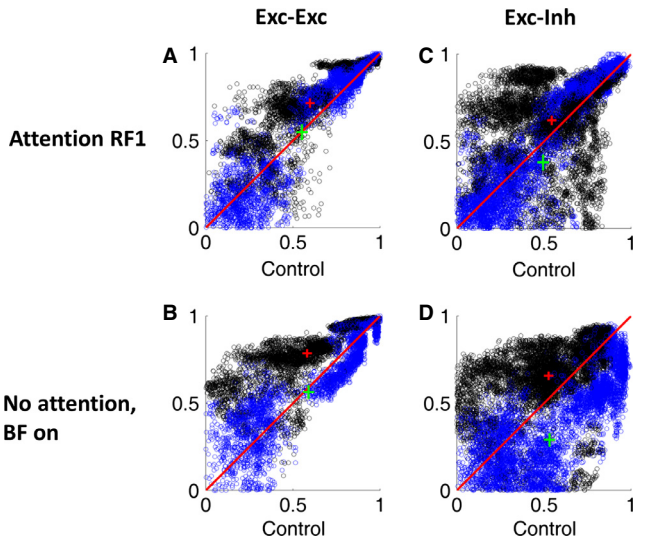

FIG. 10. Changing inhibitory spiking patterns changes interneuronal correlations. Scatter plots demonstrating how interneuronal correlations change when fast spiking inhibitory neurons in RF1 are changed to regular spiking neurons. Black and blue scatter points correspond to RF1 and RF2, respectively, and the red and green crosses correspond to their center of masses. When top-down attention is applied to RF1, both excitatory–excitatory and excitatory–inhibitory correlations increase (top, left and top, right). This is in contrast to Fig. 9A and D, in which excitatory–excitatory correlations remain constant with attention and excitatory–inhibitory correlations decrease. Similarly, when the BF is turned on (bottom) excitatory–excitatory and excitatory–inhibitory neuron correlations increase. Note that when the BF is on, RF2 (which still has fast spiking interneurons) excitatory–excitatory neuronal correlations remain constant and excitatory–inhibitory correlations decrease. This suggests that the spiking pattern of inhibitory neurons (and, thus, excitatory–inhibitory decorrelation) is necessary to sustain low levels of correlation with increases in input that accompany BF stimulation and top-down attention.

condition. A scatter point below the line $y = x$ indicates a decrease in correlation in the non-control condition. Black and blue scatter points are used for RF1 and RF2, respectively. Red and green crosses indicate the center of mass of the scatter points for RF1 and RF2, respectively, and the size of the crosses is 20 times the standard error of the mean (SEM) of the center of mass.

We first analysed the between-cell correlations during BF stimulation. A similar study was performed experimentally on rats by Goard & Dan (2009). In their study, the BF was periodically stimulated (similar to ours) while showing the rats a natural movie. They found that during periods of BF stimulation, the neurons in V1 became decorrelated. In addition, they showed that this correlation is mediated by muscarinic receptors. As can be seen in the bottom row of Fig. 8, when we stimulated the BF, excitatory–inhibitory and inhibitory–inhibitory correlations in both RF1 and RF2 decreased, while excitatory–excitatory correlations remained unchanged. Our result suggests that the decorrelation reported by Goard and Dan was primarily mediated by inhibitory neurons. For the mAChR in RF1 case (middle row of Fig. 8), we also see a decrease in between-cell correlations, indicating that the decrease in correlations is further mediated by mAChRs.

We also applied top-down attentional signals to our cortical columns and saw how this affected between-cell correlations with and without mAChR and BF stimulation (Fig. 9). Attentional modulation is classically known to increase firing rates in a particular subset of neurons in order to bias these neurons so they win out in competition against other groups (Desimone & Duncan, 1995). However, it has recently been shown that decreases in neuronal correlations via top-down signals to V4 corresponded to 80% of the attentional bias (Cohen & Maunsell, 2009; Mitchell *et al.*, 2009). In Fig. 9, we show how attention affects interneuronal correlations with and without mAChR and BF stimulation. The top row of Fig. 9 shows that when only an attentional signal is applied to RF1, excitatory–inhibitory and inhibitory–inhibitory correlations decrease, while excitatory–excitatory correlations remain constant. This decorrelation is enhanced when also stimulating mAChRs in RF1 (Fig. 9, middle). Note also in the middle row of Fig. 9 the correlations in the unattended receptive field (RF2) remain the same, indicating no bias in the unattended RF. However, when the BF is stimulated, RF2 also becomes decorrelated, resulting in a loss or weakening of this bias.

To see how the type of neuron affected interneuronal correlations within a column, we changed fast-spiking neurons in RF1 to regular-spiking neurons by changing the a and d paramaters of the Izhikevich equations (Fig. 10). When attention was applied to RF1 both excitatory–excitatory and excitatory–inhibitory correlations increase in RF1 (top row). Likewise, when the BF is activated, excitatory–excitatory and excitatory–inhibitory correlations increase in RF1 (bottom row). This implies that when an additional excitatory input drives a cortical column (e.g. top-down attention is applied to a column or the BF is activated), the firing pattern of the inhibitory neuron is crucial for maintaining low correlations. This also suggests that inhibitory neuron activation and excitation by mAChRs is perhaps a way to constrain excitatory–excitatory correlations that would arise with increased excitatory drive.

Top-down attention and BF-mediated increase in between-trial correlation

Between-trial correlation is a measure of the reliability of individual neurons in the cortex. We analysed how attention, mAChR and BF signals affect between-trial correlations by grouping single neurons into trials and computing their correlation coefficients in control and non-control conditions (similar to Figs 8 and 9) to give the between-trial correlations. For each subplot in Fig. 11, the x-axis denotes the control condition and the y-axis denotes the non-control condition. For example, the subplot in the top-left corner shows the between-trial correlations of the control condition (x-axis) against the no attention and no mAChR/BF condition (y-axis).

Top-down attentional signals may bias information in the cortex by increasing the reliability of neurons. Figure 11 (two left columns) shows that when attention was applied to RF1 and the BF was not stimulated, excitatory neurons in RF1 increased their between-trial correlation, while neurons in RF2 remained unchanged. In our model, this increase in reliability happens as a result of top-down projections to the TRN, which release TRN's inhibitory control over the LGN. We have shown a similar mechanism in a recently published computational model (Avery *et al.*, 2012a). Anatomical studies have shown that the PFC has highly topographic projections connecting to the TRN (Zikopoulos & Barbas, 2006). Because of this, the PFC can filter out distractors and up-modulate important sensory information before it even reaches the cortex. This type of attentional bias in the thalamus has been demonstrated in several studies (Crick, 1984; McAlonan *et al.*, 2006, 2008).

The BF and mAChRs are also thought to influence sensory processing. Therefore, we tested how mAChR and BF stimulation affect between-trial correlations with and without attention applied to RF1. As indicated by comparing Fig. 11D and E (excitatory neurons), mAChR stimulation in RF1 seemed to have little effect on

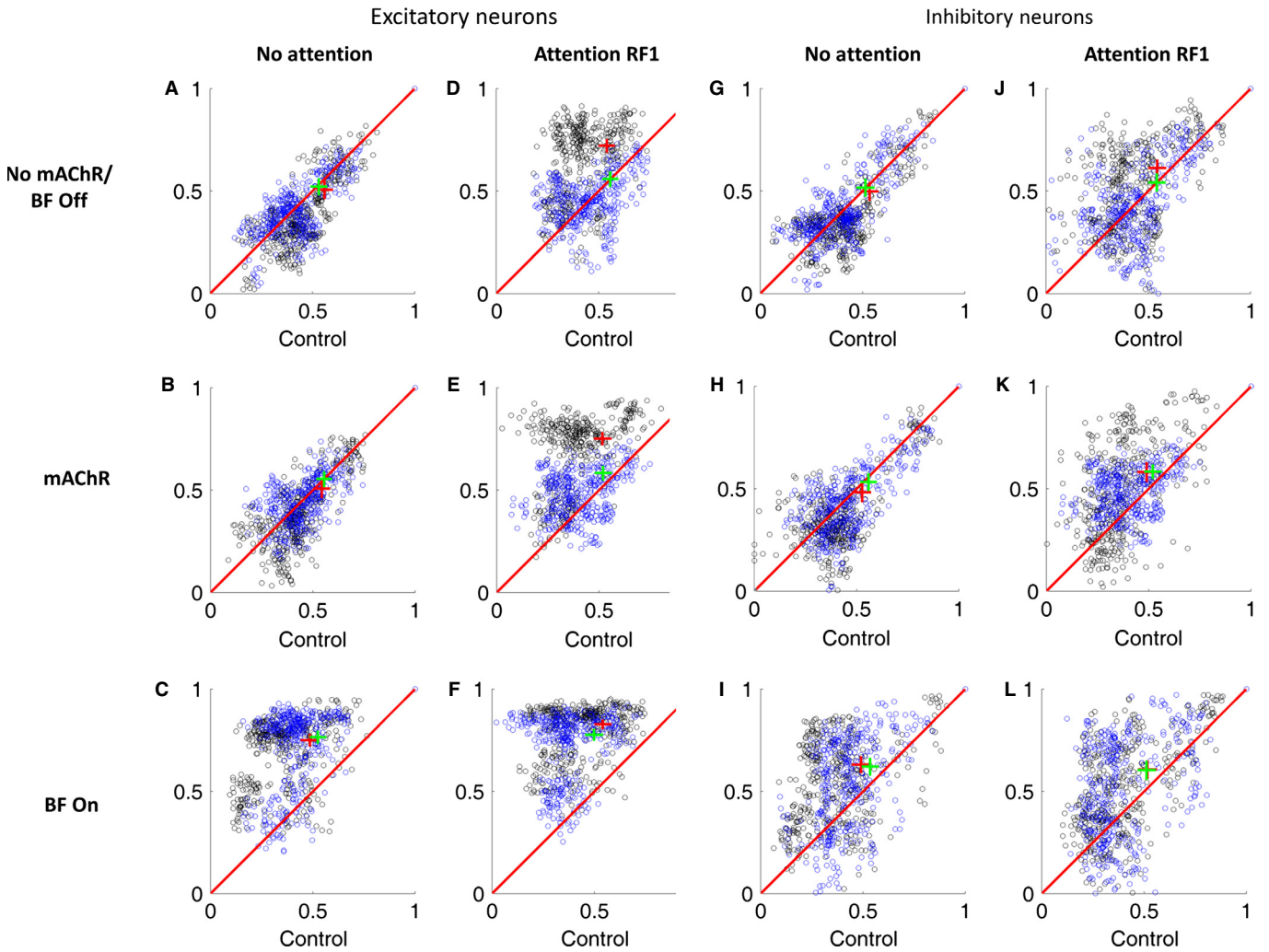

FIG. 11. Attentional and neuromodulatory effects on between-trial correlations. Scatter plots demonstrating how attention, mAChR stimulation and BF stimulation affect between-trial correlation in both excitatory (two left columns) and inhibitory (two right columns) neurons of RF1 and RF2. As in Figs 8 and 9, the red and green crosses correspond to the center of mass of the black (RF1) and blue (RF2) scatter points, respectively (size of crosses is equal to 5× ± SEM). For excitatory neurons (two left columns), between-trial correlations in RF1 increase when top-down attentional signals are applied to RF1 and the BF is off (top and middle, right columns), while the between-trial correlations in RF2 stay constant, indicating a biasing of the sensory signal to RF1. When the top-down attention is applied and the BF is stimulated (bottom figures), however, both RF1 and RF2 have an increase in between-trial correlations, indicating that the BF overrides the top-down attentional bias to RF1. For inhibitory neurons (two right columns), between-trial correlations do not show as strong of an increase in reliability in any of the cases when compared with the excitatory neurons. Note that in the bottom, right figure the red cross is beneath the green cross, making it difficult to see.

changing the reliability of the input. BF stimulation, however, was able to increase the reliability of both inputs to the cortex (Fig. 11, bottom). Goard & Dan (2009) also showed that stimulation of the BF leads to an increase in the reliability of neurons in the LGN and cortex. In addition, comparing Fig. 11E and F (excitatory neurons) shows that when the BF is stimulated, the reliability of RF2 increases to match that of RF1. This demonstrates that BF stimulation is able to override the attentional bias imposed onto RF1 and enhance both sensory inputs to the cortex. This happens as a result of GABAergic projections from the BF to the TRN, which have been shown anatomically (Bickford *et al.*, 1994). These projections make the BF very important for regulating the flow of information from the sensory periphery to the cortex. In contrast to excitatory neurons, inhibitory neurons in our simulation showed hardly any increase in reliability when top-down attention was applied (Fig. 11, inhibitory neurons) and only a weak increase in reliability when the BF was stimulated (Fig. 11I and L).

To see how the type of neuron affected between-trial correlations, we changed fast-spiking neurons in RF1 to regular-spiking neurons as above (Fig. 12). Comparing Fig. 12A–D with plots Fig. 11D, J, F and L, respectively, we see no significant changes. Thus, we can conclude that changing the spike waveform of inhibitory neurons appears not significantly to affect the between-trial correlations of either inhibitory or excitatory neurons.

Discussion

The present model illustrates several important mechanisms underlying attention and neuronal correlations in visual cortex. First, our model accounts for the BF enhancement of both bottom-up sensory input and top-down attention through 'local' and 'global' neuromodulatory circuitry. Within the context of our model, glutamatergic projections from frontal cortex synapse onto cholinergic fibers in V1, causing local cholinergic transients, which, ultimately, lead to a local

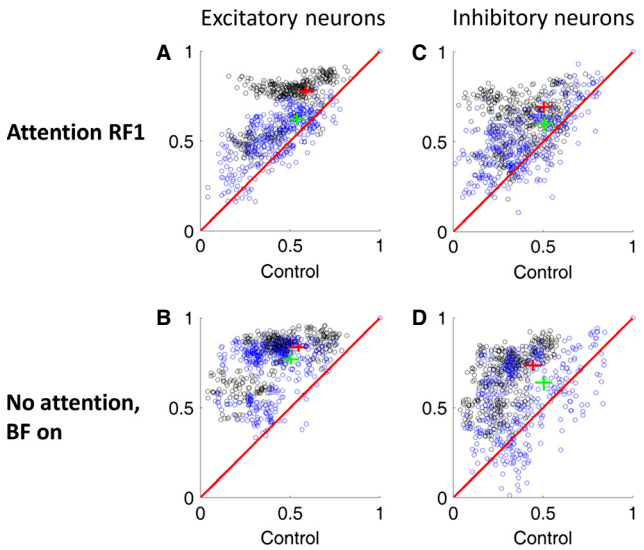

FIG. 12. Changing inhibitory spiking patterns does not significantly change between-trial correlations. Scatter plots demonstrating how between-trial correlations are affected by changing fast spiking neurons in RF1 to regular spiking neurons. When top-down attention is applied to RF1 (top), changing the firing pattern of fast spiking neurons in RF1 to regular spiking does not seem to significantly change between-trial correlations for both inhibitory and excitatory neurons (compare with Fig. 11, top row). When the BF is stimulated (bottom), both excitatory and inhibitory neurons in RF1 tend to have a slightly higher between-trial correlation (compare with Fig. 11, bottom row).

enhancement of top-down attention. In contrast, stimulation of the BF has a more global effect and can actually decrease the efficacy of top-down projections and increase sensory input by blocking top-down projections in the thalamus. Second, our model suggests an important role for mAChRs on both inhibitory and excitatory neurons. mAChRs on excitatory neurons are important for increasing firing rates and improving attentional modulation. mAChRs on inhibitory neurons, by contrast, help to maintain low levels of correlations in response to increases in excitation that come from both top-down attention and mAChRs on excitatory neurons. When excitatory drive was increased to a column due to top-down attention or BF stimulation, excitatory–inhibitory correlations decreased and excitatory–excitatory correlations remained constant. This decrease in correlations was further mediated by mAChRs. When the firing pattern of inhibitory neurons was changed from fast-spiking to regular-spiking, excitatory–excitatory and excitatory–inhibitory correlations increased with top-down attention and BF stimulation. This suggests an important role for inhibition in maintaining low excitatory–excitatory correlation levels when excitation is increased due to mAChR stimulation on excitatory neurons or added inputs, such as top-down attention.

The present model accounts for experimental results demonstrating BF's role in the enhancement of both bottom-up sensory input and top-down attention. While it has been traditionally accepted that activation of the BF cholinergic system amplifies bottom-up sensory input to the cortex while reducing cortico-cortical and top-down attention (Hasselmo & McGaughy, 2004; Yu & Dayan, 2005; Disney *et al.*, 2007), it has also been shown that ACh may be important for enhancing top-down attentional signals in visual cortex (Herrero *et al.*, 2008). To resolve these seemingly contradictory results, we propose a circuit that involves global and local modes of action by which the BF can enhance sensory and top-down attentional input, respectively. When the BF is stimulated (Fig. 13A, top), it releases ACh in V1 and disinhibits thalamic relay nuclei (via GABAergic projections to the TRN) in a non-specific manner. This leads to a global enhancement of sensory input to the cortex and may correspond to a heightened state of arousal. In contrast, when top-down attentional signals stimulate visual cortex, they can cause a local release of ACh within the context of our model, which enhances attention locally (Fig. 13A, bottom).

The exact mechanisms underlying BF enhancement of sensory information in visual cortex are not completely understood, although it has been suggested that nicotinic receptors play an important role (Disney *et al.*, 2007). We propose that this balance of bottom-up sensory input and top-down input may also be occurring at the level of the thalamus. Topographic projections from the PFC to the TRN, which bias salient input coming from the sensory periphery, may be inhibited via GABAergic projections from the BF. This gives the BF a graded control over top-down attentional biases that PFC may be having on the thalamus. We also suggest that local release of ACh modulates attention by enhancing the firing rates of attended regions in the cortex (Fig. 7). This result matches well with electrophysiological and pharmacological experiments performed on monkeys (Herrero *et al.*, 2008).

A significant finding from our model was that top-down attentional signals and simulated mAChRs decreased correlations between excitatory–inhibitory and inhibitory–inhibitory neurons in the cortex; however, excitatory–excitatory correlations remained unchanged (Figs 8 and 9). Several experimental studies have shown that attention and neuromodulation decrease interneuronal noise correlations (Cohen & Maunsell, 2009; Goard & Dan, 2009; Mitchell *et al.*, 2009). In fact, Cohen and Maunsell showed that decorrelation caused more than 80% of the attentional improvement in the population signal. This suggested that decreasing noise correlations was more important than firing rate-related biases. These studies, however, did not identify the types of neurons they were recording from, which may be difficult using conventional recording techniques.

Our model predicts that the decorrelations seen in these studies may be excitatory–inhibitory pairs of neurons rather than excitatory–excitatory pairs. In our model, we found no change in excitatory–excitatory correlations when applying top-down attention and stimulating the BF, but saw a significant decrease in excitatory–inhibitory and inhibitory–inhibitory correlations. In this view, excitatory–excitatory pairs are able to maintain a constant, low correlation state regardless of the amount of excitatory drive (which should increase correlations) due to fast-spiking inhibitory neurons (Fig. 13B). Because muscarinic receptors caused a further decrease in excitatory–inhibitory correlations, we suggest that they may act as a buffer, absorbing increases in excitation that occur with attention and BF stimulation by changing either the inhibitory spike waveform (i.e. inhibitory speed) or the inhibitory strength.

A recently published study further substantiates our finding that excitatory–inhibitory pairs of neurons have stronger decorrelation than excitatory–excitatory pairs. Middleton *et al.* (2012) were able to distinguish between excitatory and inhibitory neurons and looked at the correlations between these pairs in layer 2/3 of the rat's whisker barrel cortex. They compared correlations during spontaneous and sensory stimulated states and found that excitatory–inhibitory pairs of neurons became decorrelated when sensory stimuli were presented to the animal, whereas excitatory–excitatory pairs of neurons remained at low levels of correlations.

Our model suggests that the spiking pattern of the inhibitory neuron is important for maintaining neuronal decorrelation when further excitatory drive is applied (Fig. 10). Given excitatory–inhibitory decorrelation and minimal excitatory–excitatory correlations both in our model and in Middleton *et al.* (2012), we suggest that a primary

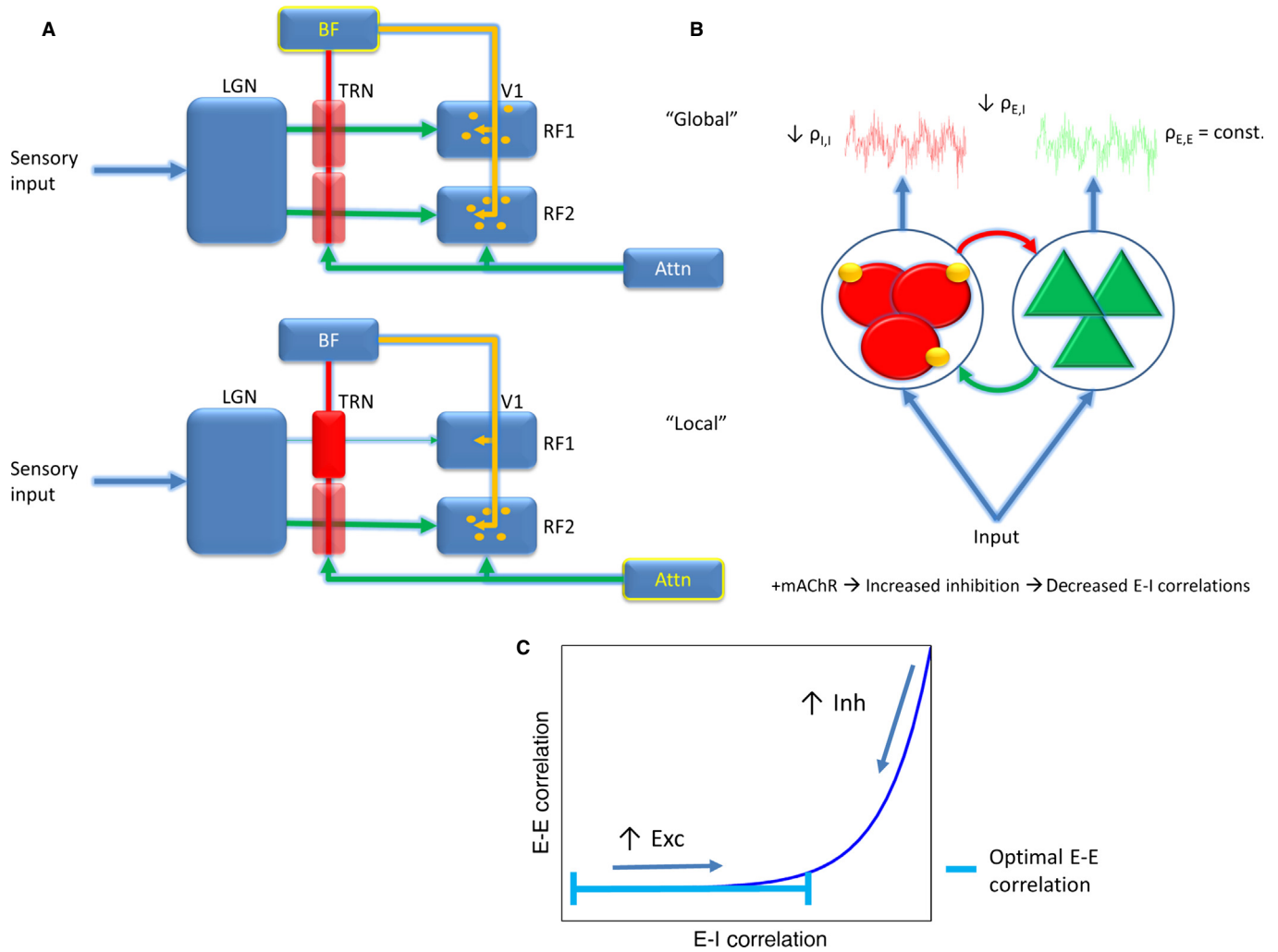

FIG. 13. Global vs. local neuromodulation and the mechanism of cholinergic-mediated decorrelation. (A) When the basal forebrain is stimulated (top), GABAergic projections from the basal forebrain inhibit neurons in the TRN, disinhibiting the LGN. This increases the reliability of all signals coming into cortex (Fig. 11). Cholinergic projections from the basal forebrain also release acetylcholine (shown in orange) non-specifically. This leads to a global enhancement of information coming into cortex and may be associated with a heightened state of arousal. This may also be a means of blocking attentional signals that may be biasing information via projections to the TRN. When attention is applied to a specific receptive field and the BF is not stimulated (bottom), the top-down projections disinhibit the LGN for a single receptive field and cause local acetylcholine release. (B) Muscarinic receptors (shown in orange) excite inhibitory neurons (red) in V1. This leads to an increase in inhibition and a decrease in correlations between excitatory–inhibitory ($\rho_{E,I}$) and inhibitory–inhibitory ($\rho_{I,I}$) neuron pairs. We propose this additional inhibition is important for keeping excitatory–excitatory correlations ($\rho_{E,E}$) low in times of increased excitatory input. (C) Plot showing the relationship that our model suggests exists between excitatory–inhibitory and excitatory–excitatory correlations. Increased excitation tends to drive both excitatory–excitatory and excitatory–inhibitory correlations up. The strength of the inhibitory drive, by contrast, fights this to maintain low decorrelations between excitatory–excitatory pairs. Low levels of inhibition due to a decrease in inhibitory strength or speed [e.g. changing the inhibitory neurons waveform (Fig. 10)] would lead to an increase in excitatory–excitatory and excitatory–inhibitory correlations. The stimulation of muscarinic receptors on inhibitory neurons may thus act as a buffer, decorrelating excitatory–inhibitory neuronal pairs to absorb increases in excitation that may otherwise cause an increase excitatory–excitatory correlations.

role of inhibitory neurons in cortex is to maintain a low level of excitatory–excitatory correlations with changing levels of excitation that may arise due to mAChR stimulation of excitatory neurons and/or top-down attentional signals. As illustrated in Fig. 13C, we propose that there is a relationship between excitatory–excitatory and excitatory–inhibitory correlations that is dependent upon levels of excitation and inhibition. Increased excitation will tend to increase correlations and increased inhibition will tend to decrease correlations between excitatory–excitatory and excitatory–inhibitory pairs. Inhibition may be important for maintaining optimal levels of excitatory–excitatory correlation in visual cortex. This implies that increasing inhibition makes it more difficult for an excitatory input to push the network out of the optimal regime and into a higher excitatory–excitatory correlation state (Fig. 13C). ACh's role in V1, then, might be to further activate inhibitory neurons so that they can absorb the increase in excitation that comes with top-down attention and BF activation of mAChRs on excitatory neurons without adding in excessive correlations.

It has been suggested that low-frequency excitatory–excitatory noise correlations originate from cortico-cortical connections (Mitchell *et al.*, 2009). It is possible that we do not see attention and mAChR-dependent decreases in excitatory–excitatory correlations, then, due to the fact that our model does not incorporate these connections. Interestingly, mAChRs have been shown to also decrease lateral connectivity in the cortex (Hasselmo & McGaughy, 2004), which could potentially mediate the decrease in excitatory–excit-

atory correlations. It would be interesting to develop a model that incorporates cortico-cortical connections to see if mAChR-dependent reductions in their efficacy can decrease noise correlations between excitatory neurons.

It is important to point out that decreases in excitatory–excitatory correlations only improve encoding when two neurons have high signal correlations (Averbeck & Lee, 2006). Because neurons in each column receive the same Gabor-filtered input, we assume they all have high signals correlations, and thus decorrelating the signal would improve coding. Neurons that have low signal correlations, by contrast, such as neurons that encode for orthogonal stimulus orientations within a single receptive field, may improve encoding by increasing noise correlations. mAChR influences on lateral connectivity strength may thus be crucial for facilitating this type of improvement in information processing. From a modeling and experimental standpoint, it will be interesting to see how mAChRs influence noise correlations when signal correlations differ.

We demonstrated that both BF and top-down attentional signals lead to an increase in cortical reliability as a consequence of their projections to the TRN. The reliability of a neuron is related to the probability that it will fire at a particular time and rate given repeated presentation of the same stimulus. In a prior model, we demonstrated that GABAergic projections from the BF are able to enhance between-trial reliability in LGN and cortex and decrease the burst-to-tonic ratio in the LGN by inhibiting TRN neurons (Avery *et al.*, 2012a). Similarly, in this model we showed that stimulation of the BF increases reliability of neurons in cortex (Fig. 11F). In addition to the GABAergic projections from the BF to the TRN, it has been shown that there exist topographic top-down projections to the TRN from the PFC (Zikopoulos & Barbas, 2007; McAlonan *et al.*, 2008). These projections may act as an attentional filter, enhancing important information at the expense of irrelevant information before this information even gets to the cortex. Given this circuitry, we were able to show that top-down attentional signals can also lead to an increase in reliability of a single receptive field via projections to the TRN (Fig. 11D).

Several computational models have been recently developed that show how neuromodulation can effect cortical processing. The SMART model (Synchronous Matching Adaptive Resonance Theory) developed by Grossberg & Versace (2008) is a spiking model that included a detailed cortical and subcortical (thalamic) circuit design as well as synaptic plasticity and cholinergic neuromodulation. Deco & Thiele (2011) also developed a model demonstrating how cholinergic activity affects the interaction between top-down attentional input and bottom-up sensory information in a cortical area. Finally, a model of the cholinergic and noradrenergic systems was developed that demonstrated how these systems track expected and unexpected uncertainty in the environment, respectively, and affect several cortical targets in order to optimise behavior (Avery *et al.*, 2012b).

The present model differed from those mentioned above in several important ways. First, it showed how non-cholinergic neurons (GABAergic) in the BF could influence subcortical structures (TRN). The three papers above, by contrast, concentrated exclusively on cholinergic neurons in the BF and their influence on the cortex. Second, our model presented a mechanism showing how the BF can enhance both bottom-up sensory input and top-down attention by incorporating local and global modes of action by the BF. Thiele and Deco, on the other hand, were interested in modeling cholinergic influences on top-down attention and Avery *et al.* were interested in modeling the cholinergic enhancement of bottom-up sensory input. It would be interesting to combine the level of detail of our model and the SMART model with the wide range of cholinergic actions that were incorporated into Deco & Thiele (2011) and Avery *et al.* (2012b).

Acknowledgements

This study was supported by the Defense Advanced Research Projects Agency (DARPA) subcontract 801888-BS, Intelligence Advanced Research Projects Activity (IARPA) via Department of the Interior (DOI) contract number D10PC20021, and NSF award number IIS-0910710. The US Government is authorised to reproduce and distribute reprints for Governmental purposes notwithstanding any copyright annotation thereon. The views and conclusions contained hereon are those of the authors and should not be interpreted as necessarily representing the official policies or endorsements, either expressed or implied, of IARPA, DOI, or the US Government.

Abbreviations

ACh, acetylcholine; BF, basal forebrain; Glu, glutamate; LGN, lateral geniculate nucleus; mAChRs, muscarinic acetylcholine receptors; PFC, prefrontal cortex; TRN, thalamic reticular nucleus; V1, primary visual cortex.

References

Averbeck, B.B. & Lee, D. (2006) Effects of noise correlations on information encoding and decoding. *J. Neurophysiol.*, **95**, 3633–3644.

Avery, M.C., Krichmar, J.L. & Dutt, N. (2012a) Spiking neuron model of basal forebrain enhancement of visual attention. *IEEE IJCNN*, **2012**, 1–8.

Avery, M.C., Nitz, D.A., Chiba, A.A. & Krichmar, J.L. (2012b) Simulation of cholinergic and noradrenergic modulation of behavior in uncertain environments. *Front. Comput. Neurosci.*, **6**, 5.

Barbas, H. & Zikopoulos, B. (2007) The prefrontal cortex and flexible behavior. *Neuroscientist*, **13**, 532–545.

Bickford, M.E., Günlük, A.E., Van Horn, S.C. & Sherman, S.M. (1994) GABAergic projection from the basal forebrain to the visual sector of the thalamic reticular nucleus in the cat. *J. Comp. Neurol.*, **348**, 481–510.

Buschman, T.J. & Miller, E.K. (2007) Top-down versus bottom-up control of attention in the prefrontal and posterior parietal cortices. *Science*, **315**, 1860–1862.

Cohen, M.R. & Maunsell, J.H. (2009) Attention improves performance primarily by reducing interneuronal correlations. *Nat. Neurosci.*, **12**, 1594–1600.

Crick, F. (1984) Function of the thalamic reticular complex: the searchlight hypothesis. *Proc. Natl. Acad. Sci. USA*, **81**, 4586–4590.

Dayan, P. & Abbott, L.F. (2001) *Theoretical Neuroscience: Computational and Mathematical Modeling of Neural Systems*. The MIT Press, Cambridge, MA.

Deco, G. & Thiele, A. (2011) Cholinergic control of cortical network interactions enables feedback-mediated attentional modulation. *Eur. J. Neurosci.*, **34**, 146–157.

Desimone, R. & Duncan, J. (1995) Neural mechanisms of selective visual attention. *Annu. Rev. Neurosci.*, **18**, 193–222.

Disney, A.A., Domakonda, K.V. & Aoki, C. (2006) Differential expression of muscarinic acetylcholine receptors across excitatory and inhibitory cells in visual cortical areas V1 and V2 of the macaque monkey. *J. Comp. Neurol.*, **499**, 49–63.

Disney, A.A., Aoki, C. & Hawken, M.J. (2007) Gain modulation by nicotine in macaque v1. *Neuron*, **56**, 701–713.

Goard, M. & Dan, Y. (2009) Basal forebrain activation enhances cortical coding of natural scenes. *Nat. Neurosci.*, **12**, 1444–1449.

Grossberg, S. & Versace, M. (2008) Spikes, synchrony, and attentive learning by laminar thalamocortical circuits. *Brain Res.*, **1218**, 278–312.

Harris, K.D. & Thiele, A. (2011) Cortical state and attention. *Nat. Rev. Neurosci.*, **12**, 509–523.

Hasselmo, M.E. & McGaughy, J. (2004) High acetylcholine levels set circuit dynamics for attention and encoding and low acetylcholine levels set dynamics for consolidation. *Prog. Brain Res.*, **145**, 207–231.

Hasselmo, M.E. & Sarter, M. (2011) Modes and models of forebrain cholinergic neuromodulation of cognition. *Neuropsychopharmacol.*, **36**, 52–73.

Herrero, J.L., Roberts, M.J., Delicato, L.S., Gieselmann, M.A., Dayan, P. & Thiele, A. (2008) Acetylcholine contributes through muscarinic receptors to attentional modulation in V1. *Nature*, **454**, 1110–1114.

Herrero, J.L., Gieselmann, M.A., Sanayei, M. & Thiele, A. (2013) Attention-induced variance and noise correlation reduction in macaque V1 is mediated by NMDA receptors. *Neuron*, **78**, 729–739.

Izhikevich, E.M. (2003) Simple model of spiking neurons. *IEEE T. Neural Networ.*, **14**, 1569–1572.
Izhikevich, E.M. (2004) Which model to use for cortical spiking neurons? *IEEE T. Neural Networ.*, **15**, 1063–1070.
Izhikevich, E.M. & Edelman, G.M. (2008) Large-scale model of mammalian thalamocortical systems. *Proc. Natl. Acad. Sci. USA*, **105**, 3593–3598.
Izhikevich, E.M., Gally, J.A. & Edelman, G.M. (2004) Spike-timing dynamics of neuronal groups. *Cereb. Cortex*, **14**, 933–944.
McAlonan, K., Cavanaugh, J. & Wurtz, R.H. (2006) Attentional modulation of thalamic reticular neurons. *J. Neurosci.*, **26**, 4444–4450.
McAlonan, K., Cavanaugh, J. & Wurtz, R.H. (2008) Guarding the gateway to cortex with attention in visual thalamus. *Nature*, **456**, 391–394.
McCormick, D.A. & Prince, D.A. (1986) Mechanisms of action of acetylcholine in the guinea-pig cerebral cortex *in vitro*. *J. Physiol.*, **375**, 169–194.
Middleton, J.W., Omar, C., Doiron, B. & Simons, D.J. (2012) Neural correlation is stimulus modulated by feedforward inhibitory circuitry. *J. Neurosci.*, **32**, 506–518.
Mitchell, J.F., Sundberg, K.A. & Reynolds, J.H. (2009) Spatial attention decorrelates intrinsic activity fluctuations in macaque area V4. *Neuron*, **63**, 879–888.
Nowak, L.G., Azouz, R., Sanchez-Vives, M.V., Gray, C.M. & McCormick, D.A. (2003) Electrophysiological classes of cat primary visual cortical neurons *in vivo* as revealed by quantitative analyses. *J. Neurophysiol.*, **89**, 1541–1566.
Richert, M., Nageswaran, J.M., Dutt, N. & Krichmar, J.L. (2011) An efficient simulation environment for modeling large-scale cortical processing. *Front. Neuroinform.*, **5**, 19.
Simoncelli, E.P. & Olshausen, B.A. (2001) Natural image statistics and neural representation. *Annu. Rev. Neurosci.*, **24**, 1193–1216.
Vigneswaran, G., Kraskov, A. & Lemon, R.N. (2011) Large identified pyramidal cells in macaque motor and premotor cortex exhibit 'thin spikes': implications for cell type classification. *J. Neurosci.*, **31**, 14235–14242.
Wagatsuma, N., Potjans, T.C., Diesmann, M. & Fukai, T. (2011) Layer-dependent attentional processing by top-down signals in a visual cortical microcircuit model. *Front. Comput. Neurosci.*, **5**, 31.
Xiang, Z., Huguenard, J.R. & Prince, D.A. (1998) Cholinergic switching within neocortical inhibitory networks. *Science*, **281**, 985–988.
Yu, A.J. & Dayan, P. (2005) Uncertainty, neuromodulation, and attention. *Neuron*, **46**, 681–692.
Zikopoulos, B. & Barbas, H. (2006) Prefrontal projections to the thalamic reticular nucleus form a unique circuit for attentional mechanisms. *J. Neurosci.*, **26**, 7348–7361.
Zikopoulos, B. & Barbas, H. (2007) Circuits formultisensory integration and attentional modulation through the prefrontal cortex and the thalamic reticular nucleus in primates. *Rev. Neuroscience.*, **18**, 417–438.